

Phase diagrams modified by interfacial penalties

T.M.Atanackovic * Y.Huo †
Z.Jelicic ‡ I.Müller §

Abstract

The conventional forms of phase diagrams are constructed without consideration of interfacial energies and they represent an important tool for chemical engineers and metallurgists. If interfacial energies are taken into consideration, it is intuitively obvious that the regions of phase equilibria must become smaller, because there is a penalty on the formation of interfaces. We investigate this phenomenon qualitatively for a one-dimensional model, in which the phases occur as layers rather than droplets or bubbles. The modified phase diagrams are shown in Chapters 3 and 4.

Keywords: Interfacial energy, phase diagrams

1 Introduction

Phase diagrams for binary mixtures of the types shown in Fig. 1 are important tools for the chemical engineer and metallurgist. Their shapes may be determined from thermodynamic arguments and it turns out that Fig. 1a is the diagram appropriate to ideal mixtures in the liquid phase and mixtures of ideal gases in the vapor phase. In both phases the mixture

*Faculty of Technical Sciences, University of Novi Sad, 21000 Novi Sad, Serbia

†Department of Mechanics, Fudan University, Shanghai 200433, China, e-mail : yzhuo@fudan.edu.cn

‡Faculty of Technical Sciences, University of Novi Sad, 21000 Novi Sad, Serbia

§Technische Universität Berlin, Thermodynamics

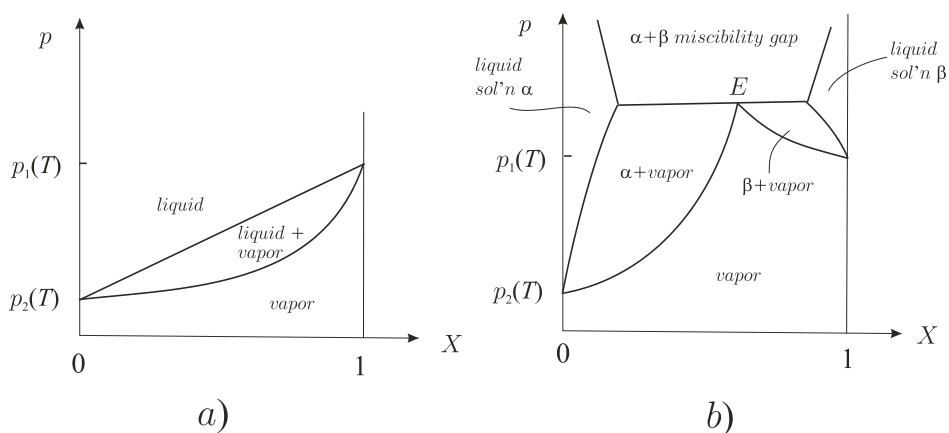


Figure 1: Prototypical binary phase diagrams with p_α T as the vapor pressures of the pure constituents $\alpha = 1$ and $\alpha = 2$. X is the mol fraction of constituent 1. a) unlimited miscibility, b) limited miscibility in the liquid phase

properties are strictly the sums of the constituent properties except for the entropies which – in both phases – contain an entropy of mixing. Fig 1b represents the more realistic case that a heat of mixing will occur, at least in the liquid phase. This means that it requires energy to mix the liquid constituents homogeneously and, if that energy is big enough, the constituents may refuse to mix except for small and large fractions X ; there is a miscibility gap.

Both types of phase diagrams in Fig. 1 ignore a potential energetic effect of the interface – or interfaces – between liquid and vapor, or between the liquid solutions α and β . And yet there *are* such energetic contributions as put in evidence by the well-known phenomena of surface tension and surface energy.

In the present paper we postulate two such energetic penalties for the formation of an interface

- an interface energy
- an energetic inhomogeneity penalty.

The former tends to decrease the number of interfaces, while the latter favors many interfaces. Both terms are forced to compromise in equilibrium.

The interfacial terms cause modifications in the shape of the phase diagrams and the goal of this study is to illustrate those modifications – at least qualitatively – for various values of the interfacial coefficients. The results are reported in Chap. 3 for the case of unrestricted miscibility and in Chap. 4 for the phase diagrams with a miscibility gap.

2 Minimizing the available free energy

2.1 Available free energy in a phase mixture

We consider a situation as shown in Fig. 2. There are two phases A and B which are both binary mixtures of the same two constituents, $\alpha = 1, 2$. This phase mixture is at temperature T and the piston exerts a pressure p . Under such circumstances the available free energy

$$\mathcal{A} = F + pV \quad (2.1)$$

tends to a minimum as equilibrium is approached. F is the Helmholtz free energy and V is the volume of the phase mixture. For mathematical simplicity we assume that the phases are layered vertically over the width of the box as shown in Fig. 2a. In Fig. 2b we see a schematic view of the fields of densities $\rho_\alpha(x)$, $\alpha = 1, 2$.

The leading term of the Helmholtz free energy is due to the free energy density $f(\rho_1, \rho_2)$, where ρ_α , ($\alpha = 1, 2$) are the mass densities of the constituents. But in the neighborhood of the phase boundaries the gradients ρ'_α of ρ_α are steep and, – according to arguments by van der Waals [1],[2] for a single constituent –, they may contribute to the energy density, thus energetically penalizing the formation of interfaces.

More recently it has been suggested by S. Müller [3] and Truskinovsky [4] that the inhomogeneity of a two-phase body should provide a contribution to the free energy. That suggestion was made in the context of an elastic bar; its extrapolation to mixtures means that the free energy density should contain terms of the type

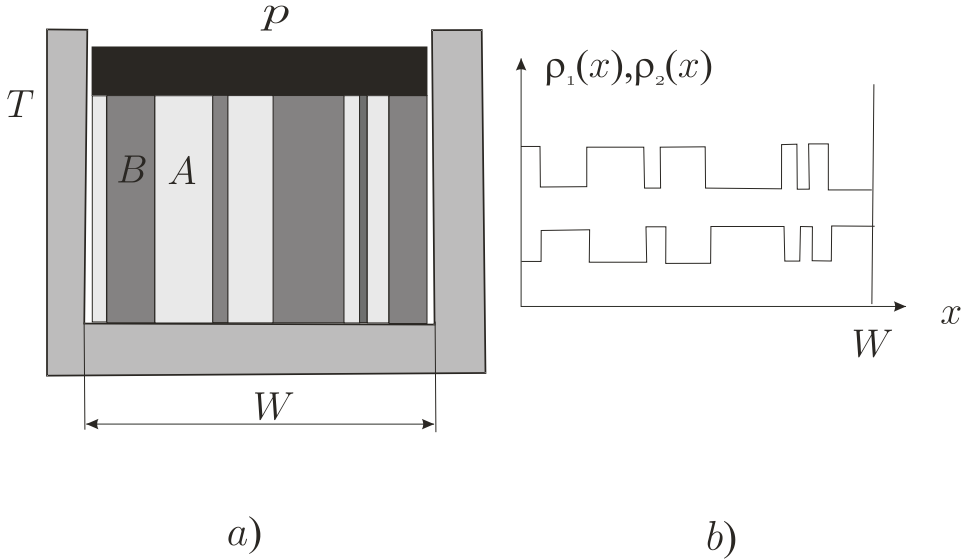


Figure 2: A phase mixture at fixed T and p . b) Schematic representation of the fields $\rho_\alpha(x)$, $\alpha = 1, 2$

$$(m_\alpha(x) - m_\alpha^0(x))^2, \quad \text{where} \quad m_\alpha(x) = \int_0^x \rho_\alpha(z) dz$$

$$m_\alpha^0(x) = m_\alpha(W) \frac{x}{W}.$$

Putting all of this together we may write the free energy in the form

$$F = \int_0^W \left\{ f(\rho_1, \rho_2) + \alpha \left([\rho_1'(x)]^2 + [\rho_2'(x)]^2 \right) + \beta \left[(m_1(x) - m_1^0(x))^2 + (m_2(x) - m_2^0(x))^2 \right] \right\} dx, \quad (2.2)$$

where α and β are positive constants. Thus the free energy is a functional of the density fields $\rho_\alpha(x)$.

The β -term represents the inhomogeneity penalty. Its form is suggested by the idea that the interfacial planes between the phases A and B have a tendency to contract so as to lower their interface energy. If they were in fact allowed to contract, the phases A and B would form menisci,

e.g. under the piston. Our 1-dimensional model, shown in Fig. 2a, forbids the menisci; therefore it implies that the interfaces are stretched. The ansatz (2.2) assumes that the energy needed for the stretching grows with the inhomogeneities $m_\alpha(x) - m_\alpha^0(x)$.

The inhomogeneity term is quite popular in the more mathematical literature, because it provides interesting problem for analysts. But even for an analyst the minimization of (2.1) with F given by (2.2) is no mean task and we avoid it altogether by assuming that the coefficients α and β are small. Let us consider this:

If α and β were both zero, the interfaces would be sharp and

- the density fields $\rho_\alpha(x)$ would be piecewise constants equal to ρ_α^A and ρ_α^B as indicated by Fig. 2b,
- the fields $(\rho'_\alpha)^2$ would be represented by δ -distributions at the N positions of the phase boundaries, and
- the inhomogeneity functions $m_\alpha(x) - m_\alpha^0(x)$ would be piecewise linear functions zig-zagging around zero.

If α and β are non-zero but small, we assume that the situation so described is essentially unchanged, so that by (2.2) we have

$$F = F_A(\rho_\alpha^A) + F_B(\rho_\alpha^B) + \tau_1 N + \text{inhomogeneity penalty}$$

Thus – for given values of the densities $\rho_\alpha^A, \rho_\alpha^B$, and of the volume fraction $z_v = V_A/V$ of phase A , and of the number of interfaces N – the available free energy assumes a minimum, when the inhomogeneity penalty is minimal. In [5] it has been proved¹ that this is the case when all A -layers and all B -layers are equally wide. In that case the inhomogeneity penalty I_N assumes the form

$$I_N = \frac{\tau_2}{2} \frac{[z_v(1-z_v)]^2}{N^2} V^3.$$

Thus the available free energy reduces to a function of only 6 variables – viz. $\rho_\alpha^A, \rho_\alpha^B, N$, and z_v –, plus p and T and we obtain

¹The identical problem arose in [5] for the case of an elastic bar, so the analysis is identical.

$$\mathcal{A} = F_A + F_B + \tau_1 N + \frac{\tau_2 [z_v (1 - z_v)]^2}{2 N^2} V^3 + pV. \quad (2.3)$$

τ_1 and τ_2 are positive constants which replace α and β of (2.2). We refer to the terms τ_1 and τ_2 as the interfacial energy and the inhomogeneity penalty respectively. Note that the former favors few interfaces while the latter favors many interfaces. The phase mixture has to compromise between the two terms and thus find the equilibrium size of the stripes of phases A and B .

We introduce molar quantities by referring \mathcal{A} to the number $\nu = \nu_A + \nu_B$ of mols. We define

$$\begin{aligned} a &= \frac{\mathcal{A}}{\nu}, & v &= \frac{V}{\nu}, & f_A &= \frac{F_A}{\nu_A}, & f_B &= \frac{F_B}{\nu_B}, \\ v_A &= \frac{V_A}{\nu_A}, & v_B &= \frac{V_B}{\nu_B}, & z &= \frac{\nu_A}{\nu}, & n &= \frac{N}{\nu}, \end{aligned}$$

and obtain

$$a = z f_A(v_A, X_A, T) + (1 - z) f_B(v_B, X_B, T) + \tau_1 n \quad (2.4)$$

$$+ \frac{\tau_2}{2} v^3 \left[\frac{z \frac{v_A}{v} (1 - z) \frac{v_B}{v}}{n} \right]^2 + pv. \quad (2.5)$$

Note that the molar fraction z is different from the volume fraction z_v . We have $z_v = z \frac{v_A}{v}$. The molar free energies f_A and f_B depend on the molar volumes v_A or v_B and on the mol fractions $X_A = \frac{\nu_A^1}{\nu_A}$, or $X_B = \frac{\nu_B^1}{\nu_B}$, and on temperature T . The preference of molar volumes and mol fractions over mass densities and mass fractions, or concentrations is inherent in the chemical-thermodynamic nature of this paper.

Equation (2.5) renders explicit the 6 variables on which the molar availability depends, viz. v_A, v_B, X_A, X_B and n, z . The molar volume v is given by

$$v = z v_A + (1 - z) v_B. \quad (2.6)$$

In addition there are 3 parameters, viz. p and T and X , the overall mol fraction of constituent 1. We have

$$X = z X_A + (1 - z) X_B. \quad (2.7)$$

2.2 Partial equilibria for fixed values of p and T

We minimize a in (2.5) under the condition of fixed p and T and by taking the constraints (2.6), (2.7) into consideration. The constraint (2.6) is considered by elimination of v , whereas the constraint (2.7) is taken care of by a Lagrange multiplier μ . Thus, we minimize

$$\Psi = a - \mu (zX_A + (1 - z) X_B). \quad (2.8)$$

It is convenient to distinguish between conditions for

- *mechanical equilibrium*, obtained by setting the derivatives of Ψ with respect to v_A and v_B equal to zero,
- *mixing equilibrium* obtained by setting the derivatives of Ψ with respect to X_A and X_B equal to zero,
- *interface equilibrium* obtained by setting the derivative of Ψ with respect to n equal to zero
- *phase equilibrium* obtained by setting the derivative of Ψ with respect to z equal to zero.

2.3 Mechanical equilibrium

The conditions for mechanical equilibrium provide

$$\begin{aligned} \frac{\partial \Psi}{\partial v_A} &= z \frac{\partial f_A}{\partial v_A} + pz \\ &+ \tau_2 \left(\frac{(1-z)v_B}{n} \right)^2 \frac{zv_A}{v} \left(1 - \frac{zv_A}{2v} \right) z = 0, \\ \frac{\partial \Psi}{\partial v_B} &= (1-z) \frac{\partial f_B}{\partial v_B} + p(1-z) \\ &+ \tau_2 \left(\frac{zv_A}{n} \right)^2 \frac{(1-z)v_B}{v} \left(1 - \frac{(1-z)v_B}{2v} \right) (1-z) = 0. \end{aligned} \quad (2.9)$$

Remembering that $-\left(\frac{\partial f_A}{\partial v_A}\right)_{X_A, T}$ and $-\left(\frac{\partial f_B}{\partial v_B}\right)_{X_B, T}$ equal the pressures p_A and p_B of the two phases we conclude from (2.9)

$$\begin{aligned} p_A &= p + \tau_2 \left(\frac{(1-z)v_B}{n} \right)^2 \frac{zv_A}{v} \left(1 - \frac{zv_A}{2v} \right), \\ p_B &= p + \tau_2 \left(\frac{zv_A}{n} \right)^2 \frac{(1-z)v_B}{v} \left(1 - \frac{(1-z)v_B}{2v} \right). \end{aligned} \quad (2.10)$$

Thus the pressures of the phases differ because of the energy penalty due to inhomogeneity, – the term with τ_2 –, even in the present one-dimensionally layered arrangement of phases.

Multiplication of (2.10)₁ by zv_A and (2.10)₂ by $(1-z)v_B$ and summation provides

$$zp_A v_A + (1-z)p_B v_B - pv = 3 \frac{\tau_2}{2} v^3 \left(\frac{z \frac{v_A}{v} (1-z) \frac{v_B}{v}}{n} \right)^2. \quad (2.11)$$

If we introduce W_A and $W_B = W - W_A$ as the total widths of the phases A and B we may write this expression in the form

$$p_A W_A + p_B W_B - \frac{3}{2} \tau_2 \frac{1}{v^2} W \left(\frac{z \frac{v_A}{v} (1-z) \frac{v_B}{v}}{n} \right)^2 = pW \quad (2.12)$$

which shows that the forces on the piston exerted by the pressures p_A, p_B and p are not balanced. The balance needs a downward force on the piston which we may think of as acting in the phase boundaries. We may conjecture that the A and B stripes of Fig. 1a tend to form concave menisci so that, when those are prevented by the one-dimensionality of our model, the phase boundaries are lengthened and thus pull the piston downwards.

2.4 Equilibrium of mixing

The conditions of mixing equilibrium read

$$\frac{\partial \Psi}{\partial X_A} = z \frac{\partial f_A}{\partial X_A} - z \mu = 0$$

$$\text{hence } \mu = \frac{\partial f_A}{\partial X_A} = \frac{\partial f_B}{\partial X_B}$$

$$\frac{\partial \Psi}{\partial X_B} = (1 - z) \frac{\partial f_B}{\partial X_B} - (1 - z) \mu = 0. \quad (2.13)$$

We recall that $\frac{\partial f_A}{\partial X_A}$ and $\frac{\partial f_B}{\partial X_B}$ equal the chemical potential differences $\mu_1^A - \mu_2^A$ and $\mu_1^B - \mu_2^B$ of the two phases and conclude that those differences are equal in mixing equilibrium

$$\mu = \mu_1^A - \mu_2^A = \mu_1^B - \mu_2^B. \quad (2.14)$$

We also recall that $\frac{\partial f_A(v_A, X_A, T)}{\partial X_A} = \frac{\partial g_A(p_A, X_A, T)}{\partial X_A}$, where $g = f + pv$ is the molar Gibbs free energy. Analogous conditions hold for phase B and therefore (2.13)₃ may be written as

$$\mu = \frac{\partial g_A(p_A, X_A, T)}{\partial X_A} = \frac{\partial g_B(p_B, X_B, T)}{\partial X_B}. \quad (2.15)$$

2.5 Interface equilibrium

Interface equilibrium requires

$$\frac{\partial \Psi}{\partial n} = \tau_1 - \tau_2 v^3 \frac{\left[z \frac{v_A}{v} (1 - z) \frac{v_B}{v} \right]^2}{n^3} = 0. \quad (2.16)$$

Hence follows for the equilibrium molar number n of interfaces

$$n = \sqrt[3]{\frac{\tau_2}{\tau_1} \frac{1}{v^{1/3}} [z v_A (1 - z) v_B]^2}. \quad (2.17)$$

If mechanical *and* interface equilibrium prevail, (2.10) with (2.17) provide

$$\begin{aligned} p_A &= p + \sqrt[3]{\tau_1^2 \tau_2} \frac{[(1 - z) v_B]^{2/3}}{(z v_A)^{1/3} v^{1/3}} \left(1 - \frac{z v_A}{2v} \right), \\ p_B &= p + \sqrt[3]{\tau_1^2 \tau_2} \frac{[z v_A]^{2/3}}{[(1 - z) v_B]^{1/3} v^{1/3}} \left(1 - \frac{(1 - z) v_B}{2v} \right), \end{aligned} \quad (2.18)$$

so that p_A becomes very large when z becomes small and p_B becomes large when z approaches 1.

Once again for mechanical and interface equilibrium we may use (2.16) to eliminate τ_1 from the molar available free energy a and then use (2.11) to obtain

$$a = zg_A(p_A, X_A, T) + (1 - z)g_B(p_B, X_B, T). \quad (2.19)$$

Thus the available free energy of the phase mixture is the weighted sum of the Gibbs free energies of the phases with the phase fractions as weighting factors. In particular there is no explicit term due to interfacial energy or inhomogeneity energy. It is true though that p_A and p_B , the pressure arguments in g_A and g_B are determined by τ_2 and τ_1 , cf. (2.18).

2.6 Phase equilibrium

We obtain the phase equilibrium from

$$\begin{aligned} \frac{\partial \Psi}{\partial z} = & f_A - f_B \\ & + \tau_2 \frac{v_A^2 v_B^2}{n^2 v} \left\{ \underline{z(1-z)(1-2z) - \frac{v_A - v_B}{2v} [z(1-z)]^2 + p(v_A - v_B)} \right\} \\ & - \mu(X_A - X_B) = 0. \end{aligned}$$

The underlined part is simply given by $p_A v_A - p_B v_B$ provided that mechanical equilibrium prevails so that we have

$$g_A(p_A, X_A, T) - g_B(p_B, X_B, T) = \mu(X_A - X_B). \quad (2.20)$$

By the condition (2.15) of mixing equilibrium we may write (2.20) in the form

$$\mu = \left(\frac{\partial g_A}{\partial X_A} \right)_{p_A, T} = \left(\frac{\partial g_B}{\partial X_B} \right)_{p_B, T} = \frac{g_A(p_A, X_A, T) - g_B(p_B, X_B, T)}{X_A - X_B}. \quad (2.21)$$

This is the well-known prescription for finding the mol fractions X_A and X_B in equilibrium as abscissae of the contact points of the common tangent of the curves g_A and g_B . Such a graphical construction of X_A and

X_B is reported in many textbooks, even though these may not account for different pressures p_A, p_B and p .

The only difference here to the standard procedure is that the common tangent must be drawn to the molar Gibbs free energies pertaining to different pressures, viz. p_A and p_B .

With the same qualification we recover the Gibbs phase rule by which the chemical potentials of all constituents are equal in all phases in equilibrium. This can be concluded from (2.13) and (2.21)₃ by remembering that $g_A = X_A \mu_1^A + (1 - X_A) \mu_2^A$ and $g_B = X_B \mu_1^B + (1 - X_B) \mu_2^B$. It follows

$$\mu_1^A(p_A, X_A, T) = \mu_1^B(p_B, X_B, T) \quad \text{and}$$

$$\mu_2^A(p_A, X_A, T) = \mu_2^B(p_B, X_B, T). \quad (2.22)$$

Once again we must realize that the equal chemical potentials refer to different pressures in phases A and B .

It must also be realized that the final equilibrium conditions (2.22) are two in number, but they are conditions on five variables, viz. p_A, p_B, T , and X_A, X_B , or – by (2.18) – on p, T, z, X_A, X_B . We conclude that phase equilibrium leaves us with three degrees of freedom, – rather than two, when $\tau_1 \tau_2 = 0$. Therefore the interfacial terms require a modification of the Gibbs phase rule.

3 Nucleation and formation of kernels

3.1 Analytic constitutive equations for the phases

We assume that both phases are ideal mixtures with molar volumes v_α^A and v_α^B ($\alpha = 1, 2$) for the pure constituents under the pressures p_A or p_B respectively. This means that we have

$$v^A = X_A v_1^A + (1 - X_A) v_2^A \quad \text{and} \quad v^B = X_B v_1^B + (1 - X_B) v_2^B. \quad (3.1)$$

The assumption of ideal mixtures also implies that g_A and g_B may be written in the forms

$$\begin{aligned} g_A(p_A, X_A, T) &= X_A (g_1^A(p_A, T) + RT \ln X_A) \\ &\quad + (1 - X_A) (g_2^A(p_A, T) + RT \ln(1 - X_A)), \\ g_B(p_B, X_B, T) &= X_B (g_1^B(p_B, T) + RT \ln X_B) \\ &\quad + (1 - X_B) (g_2^B(p_B, T) + RT \ln(1 - X_B)), \end{aligned} \quad (3.2)$$

where $g_\alpha^A(p_A, T)$ and $g_\alpha^B(p_B, T)$ ($\alpha = 1, 2$) are the molar Gibbs free energies of the pure constituents α under the pressures p_A and p_B respectively; the logarithmic terms represent the entropies of mixing.

Of phase A we assume that it is ideal mixture of incompressible liquids. In that case v_α^A ($\alpha = 1, 2$) are constants and $g_\alpha^A(p_A, T)$ are linear functions of p_A . It is convenient to write $g_\alpha^A(p_A, T) = g_\alpha^A(p_\alpha(T), T) + v_\alpha^A(p_A - p_\alpha(T))$, thereby referring $g_\alpha^A(p_A, T)$ to the saturation vapor pressure $p_\alpha(T)$ of constituent α . Thus we obtain

$$\begin{aligned} g_A(p_A, X_A, T) &= X_A (g_1^A(p_1(T), T) + v_1^A(p_A - p_1(T)) + RT \ln X_A) \\ &\quad + (1 - X_A) (g_2^A(p_2(T), T) \\ &\quad + v_2^A(p_A - p_2(T)) + RT \ln(1 - X_A)), \end{aligned} \quad (3.3)$$

Of phase B we assume that it is a mixture of ideal gases so that $v_\alpha^B = \frac{1}{p_B} RT$ ($\alpha = 1, 2$) holds. $g_\alpha^B(p_B, T)$ ($\alpha = 1, 2$) are then logarithmic functions of p_B and again it is convenient to refer them to the saturation vapor pressures $p_\alpha(T)$. Thus $g_B(p_B, X_B, T)$ reads

$$\begin{aligned} g_B(p_B, X_B, T) &= X_B (g_1^B(p_1(T), T) + RT \ln \left[\frac{p_B}{p_1(T)} X_B \right]) \\ &\quad + (1 - X_B) (g_2^B(p_2(T), T) \\ &\quad + RT \ln \left[\frac{p_B}{p_2(T)} (1 - X_B) \right]). \end{aligned} \quad (3.4)$$

The chemical potentials of the constituents α in the two phases are given by

$$\begin{aligned} \mu_\alpha^A &= g_\alpha^A(p_\alpha(T), T) + v_\alpha^A(p_A - p_\alpha(T)) \\ &\quad + \begin{cases} RT \ln X_A & \alpha = 1 \\ RT \ln(1 - X_A) & \alpha = 2 \end{cases} \end{aligned}$$

$$\mu_{\alpha}^B = g_{\alpha}^B(p_{\alpha}(T), T) + \begin{cases} RT \ln \left[\frac{p_B}{p_{\alpha}(T)} X_B \right] & \alpha = 1 \\ RT \ln \left[\frac{p_B}{p_{\alpha}(T)} (1 - X_B) \right] & \alpha = 2 \end{cases} \quad (3.5)$$

In the sequel we shall present diagrams, – usually as the results of numerical evaluations. The specific values of the material parameters which we use in those calculations are those appropriate for a mixture of propane and butane and they all refer to $T = 293K$.

The molar volumes of the pure liquids are

$$v_1^A = 75.24 \times 10^{-6} \frac{\text{m}^3}{\text{mol}} \quad v_2^A = 96.86 \times 10^{-6} \frac{\text{m}^3}{\text{mol}} \quad (3.6)$$

and the saturation vapor pressures are

$$p_1(T) = 8.288 \text{ bar} \quad p_2(T) = 2.064 \text{ bar} \quad (3.7)$$

respectively for propane and butane. The values for τ_1 and τ_2 are unknown and we choose them so as to clearly emphasize the possible effects of the penalties.

3.2 Analytic available energy for the phase mixture in mechanical and interface equilibrium

With the specific constitutive relations (3.3), (3.4) we may write the available free energy (2.19) of the phase mixture in mechanical and interface equilibrium in the form

$$\begin{aligned} a = & z \left\{ X_A (g_1^A(p_1(T), T) + v_1^A(p_A - p_1(T)) + RT \ln X_A) \right. \\ & + (1 - X_A) (g_2^A(p_2(T), T) + v_2^A(p_A - p_2(T)) + RT \ln(1 - X_A)) \left. \right\} \\ & + (1 - z) \left\{ X_B (g_1^B(p_1(T), T) + RT \ln \left[\frac{p_B}{p_1(T)} X_B \right]) \right. \\ & \left. + (1 - X_B) (g_2^B(p_2(T), T) + RT \ln \left[\frac{p_B}{p_2(T)} (1 - X_B) \right]) \right\}. \quad (3.8) \end{aligned}$$

The convenience in referring to the saturation vapor pressures $p_\alpha(T)$ becomes now obvious: it allows us to use the fact that $g_\alpha^A(p_\alpha(T), T) = g_\alpha^B(p_\alpha(T), T)$ holds. Therefore we have

$$\begin{aligned}
a - Xg_1^A(p_1(T), T) - (1 - X)g_2^A(p_2(T), T) \\
= z \{ X_A v_1^A (p_A - p_1(T)) + (1 - X_A) v_2^A (p_A - p_2(T)) \\
+ RT(X_A \ln X_A + (1 - X_A) \ln(1 - X_A)) \} \\
+ (1 - z) \left\{ X_B RT \ln \left[\frac{p_B}{p_1(T)} \right] + (1 - X_B) RT \ln \left[\frac{p_B}{p_2(T)} \right] \right. \\
\left. + RT [X_B \ln X_B + (1 - X_B) \ln(1 - X_B)] \right\}. \quad (3.9)
\end{aligned}$$

In particular for $z = 0$ and $z = 1$ this equation implies the Gibbs free energies for the single phases B and A respectively. For $z = 0$ we have with $X = X_B$ and $p_B = p$, cf. (2.10), or (2.18)

$$\begin{aligned}
a_{z=0} - Xg_1^A(p_1(T), T) - (1 - X)g_2^A(p_2(T), T) = \\
RT \left\{ X \ln \frac{p}{p_1(T)} + (1 - X) \frac{p}{p_2(T)} + [X \ln X + (1 - X) \ln(1 - X)] \right\}. \quad (3.10)
\end{aligned}$$

For $z = 1$ we have with $X_A = X$ and $p_A = p$

$$\begin{aligned}
a_{z=1} - Xg_1^A(p_1(T), T) - (1 - X)g_2^A(p_2(T), T) \\
= RT \left\{ X \frac{(p - p_1(T)) v_1^A}{RT} + (1 - X) \frac{(p - p_2(T)) v_2^A}{RT} \right. \\
\left. + [X \ln X + (1 - X) \ln(1 - X)] \right\}. \quad (3.11)
\end{aligned}$$

3.3 Available free energy for the phase mixture in mechanical and interface equilibrium and equilibrium of mixing

If in addition to mechanical and interface equilibrium we also have equilibrium of mixing, the chemical potential differences must be equal in

both phases cf. (2.13), (2.14). By (3.5) this condition implies for the present simple constitutive equations

$$\ln \left(\frac{X_A}{1 - X_A} \frac{1 - X_B}{X_B} \right) = \ln \frac{p_2(T)}{p_1(T)} + \frac{(p_A - p_2(T)) v_2^A}{RT} - \frac{(p_A - p_1(T)) v_1^A}{RT}. \quad (3.12)$$

Also, of course we must have

$$zX_A + (1 - z)X_B = X. \quad (3.13)$$

These are two relations from which – for given values of p and T – we may determine

$$X_A = X_A(z, X) \quad \text{and} \quad X_B = X_B(z, T). \quad (3.14)$$

The actual determination of these functions must be done numerically, because by (2.18) the pressures p_A and p_B depend on z and X_A, X_B in a very complex manner. [Recall that $v_A = X_A v_1^A + (1 - X_A) v_2^A$ holds and $v_B = \frac{RT}{p_B}$; also $v = z v_A + (1 - z) v_B$].

To give an impression of the ensuing functions $X_A = X_A(z, X)$ and $X_B = X_B(z, X)$ we draw the corresponding graphs for *one* value of the parameter X , viz. $X = 0.6$. Fig. 3 shows the graphs. Obviously we must have $X_A = 0.6$ for $z = 1$ and $X_B = 0.6$ for $z = 0$. Both functions increase with z , *but not linearly, as would be expected if* τ_1 and τ_2 were equal to zero. All plots in this chapter employ the values $\tau_1 = 20 \cdot 10^4 J$ and $\tau_2 = 20 \cdot 10^4 J/m^9$ and all numbers are calculated with those values.

In a process of condensation by an increase of pressure the liquid fraction X_A starts low with a 2-rich liquid with $X_A \approx 0.27$ and moves up to $X_A = 0.6$ as the condensation is completed; analogously the condensation starts with a vapor fraction $X_B = 0.6$ and during the process the residual vapor is enriched in constituent 1 up to a value $X_B \approx 0.85$.

Once the mol fractions X_A and X_B in the two phases have thus been determined numerically we may use (3.14) to eliminate those mol fractions from the available free energy a in (3.9). We thus obtain $a = a(z; X, p, T)$. For a given pair $(p, T) = (5 \text{ bar}, 293 \text{ K})$ and for $X = 0.6$ Fig. 4a shows that available free energy a as a function of z . Actually the plot of the figure is for the function

$$\tilde{a} = a - X g_1^A(p_1(T), T) - (1 - X) g_2^A(p_2(T), T),$$

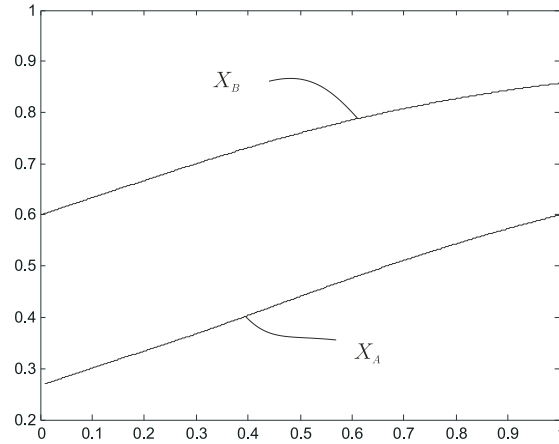


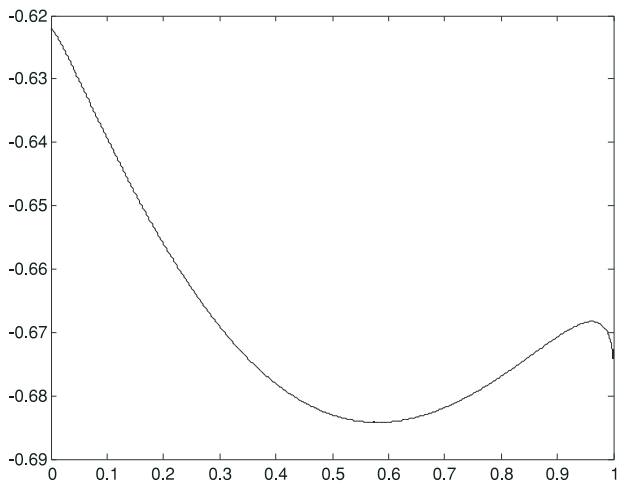
Figure 3: The equilibrium mol fractions of phases A and B for $X=0.6$ as function of the liquid fraction z

i.e. the right hand side of (3.9). We call this function the *reduced* availability. In Fig. 4b we show an enlarged plot of the diagram, for small values of z .

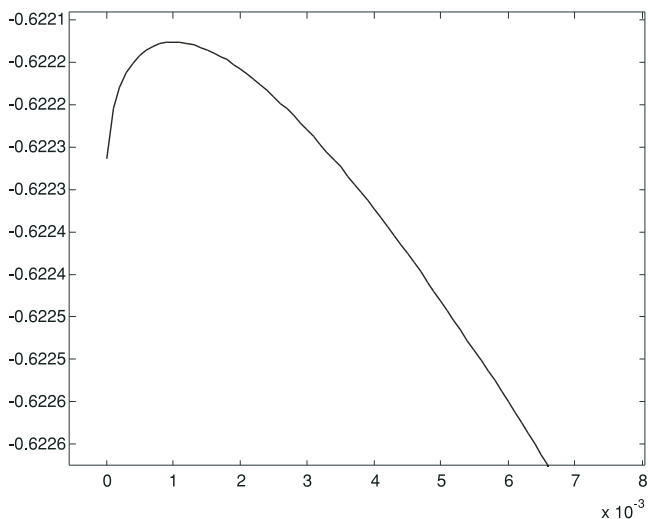
Inspection of Figs.4a and 4b shows that the function $\tilde{a}(z)$ has five extrema. The lateral ones are end-point-minima corresponding to the pure phases $z = 0$ and $z = 1$. The middle minimum corresponds to a phase mixture with $z \approx 0.519$. In-between those minima we have barriers which we must interpret as nucleation barriers. True mechanical, interface- and mixing-equilibrium occurs for *the* one of the three minima which has the smallest value of \tilde{a} . In Fig. 4a that is the middle minimum with $z \approx 0.519$ and – according to Fig. 3 – $X_A \approx 0.45$ and $X_B \approx 0.76$. When this phase mixture prevails, the nucleation barriers must have been overcome; that can happen in a fluctuation or by interference from outside introduced by shaking or stirring.

3.4 Nucleation barriers

The situation is not unlike the case of a droplet forming in a vapor, or a bubble in a liquid, cases which were originally treated by W. Thomson (Lord Kelvin) [6]. Generally the interpretation is that in a homogeneous



(a) $p = 5bar, T = 293K, X = 0.6$



(b) $p = 5bar, T = 293K, X = 0.6$ in the neighborhood

Figure 4: The reduced availability in units of RT in mechanical equilibrium, interface equilibrium and equilibrium of mixing as a function of phase fraction z .

phase the barrier must be overcome by a fluctuation; if a fluctuation in the vapor phase $z = 0$ creates a liquid nucleus with the phase fraction corresponding to the left maximum, that nucleus will grow until it reaches the middle minimum. The middle minimum will also be reached after formation of a sufficiently big vapor nucleus in the liquid phase $z = 1$.

The nucleation barriers are the energetic differences between the maxima and the lateral minima in Fig. 4. The barriers for the emergence of liquid in vapor and of vapor in liquid are, – always for $X = 0.6$

$$\Delta a_L = 1.25 \cdot 10^{-4} RT \quad \text{and} \quad \Delta a_V = 59.4 \cdot 10^{-4} RT$$

respectively and the corresponding phase fractions are

$$z_{\max}^L = 1 \cdot 10^{-3} \quad \text{and} \quad z_{\max}^V = 0.96.$$

In a manner of speaking we may call z_{\max}^L the phase fraction of the critical droplet, while z_{\max}^V is the phase fraction of the critical bubble. Note, however that the one-dimensionality of our mathematical model makes it difficult to think of the nuclei as droplets or bubbles.

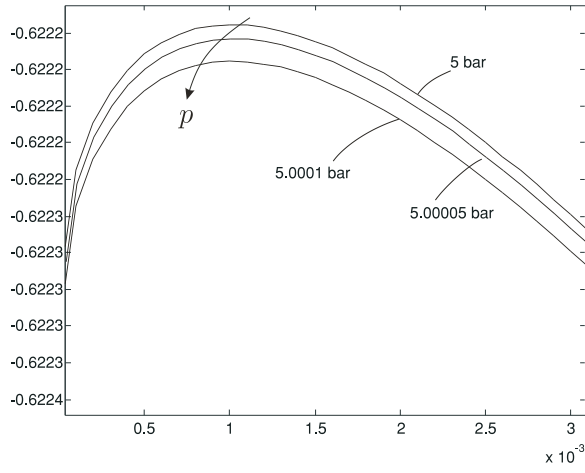
The size of the barriers depends on the pressure in such a way that Δa_V becomes bigger and Δa_L becomes smaller as the pressure increases. Figs. 5a and 5b illustrate that effect by showing plots of \tilde{a} in the vicinity of the pure phases for three pressures, viz. 5.0 bar, 5.00005 bar and 5.0001 bar in the vicinity of vapor phase and 5.0 bar, 5.025 bar and 5.05 bar in the vicinity of liquid phase.

However, the nucleation barriers never disappear, irrespective of pressure.

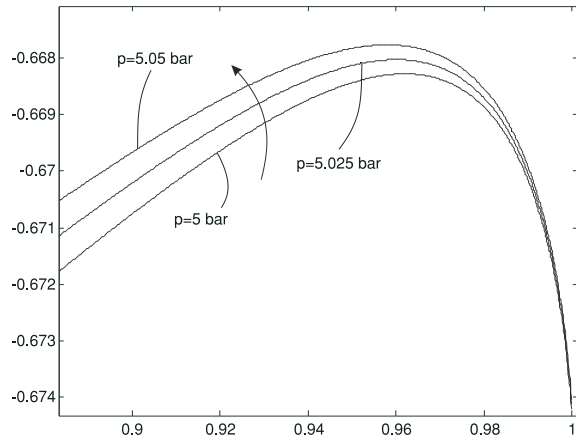
All graphs and values reported in Sects 3.3 and 3.4 refer to the value $X = 0.6$. Corresponding graphs and values must be known – and have been calculated – for all X between 0 and 1, and they will be used in the sequel.

3.5 Full equilibrium

In addition to mechanical and mixing equilibrium and interface equilibrium we now allow phase equilibrium to prevail so that the chemical potentials satisfy the conditions $\mu_\alpha^A = \mu_\alpha^B$ ($\alpha = 1, 2$), cf (2.22). Because of



(a) Reduced availability in the neighborhood of the pure vapor phase



(b) Reduced availability in the neighborhood of the pure liquid phase

Figure 5:

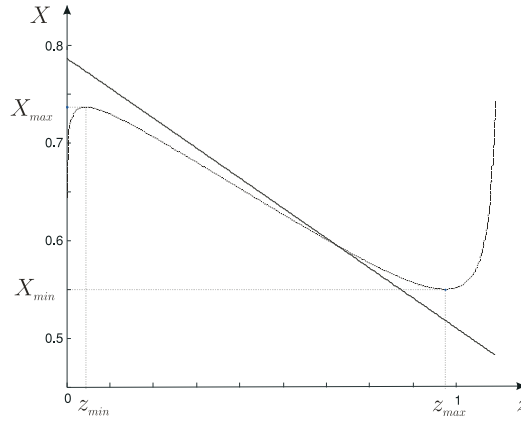


Figure 6: $X=X(z)$ for the pair $(p,T)=(5\text{bar}, 293\text{K})$ with penalties τ_1, τ_2 (dotted) and without penalties (solid). See Fig.8 for the significance of the coordinates of the extrema

(2.14), which ensures mixing equilibrium, this represents *one* additional condition, e.g. $\mu_1^A = \mu_1^B$, or by (3.5) with $g_1^A(p_1(T), T) = g_1^B(p_1(T), T)$

$$v_1^A(p_A - p_1(T)) + RT \ln X_A = RT \ln \frac{p_B}{p_1(T)} + RT \ln X_B \quad (3.15)$$

We already have $X_A(X, z)$ and $X_B(X, z)$ cf. (3.14) and, by (2.18), p_A and p_B are also known functions of X and z . Thus for a given pair (p, T) (3.15) provides a relation between X and z . This relation can be obtained numerically and Fig. 6 represents the function $X = X(z)$ in the form of the non-monotone graph in that figure.

The solid line in Fig. 6 represents the function $X = X(z)$, if neither interface nor inhomogeneity penalties exist. In this case (3.12) and (3.13) imply that $X(z)$ is a linear function.

When we insert the conditions (3.14) of mixing equilibrium into the reduced availability \tilde{a} (3.9) and use the condition (3.15) of phase equilibrium to eliminate z , we obtain three branches for $\tilde{a}_E(X, p, T)$, i.e. \tilde{a} in full equilibrium. Those three branches correspond to the three monotone parts of the functions $X = X(z)$ in Fig. 6 and they form a loop as shown in Fig. 7 for $(p, T) = (5 \text{ bar}, T=298 \text{ K})$. The lower part of the loop is

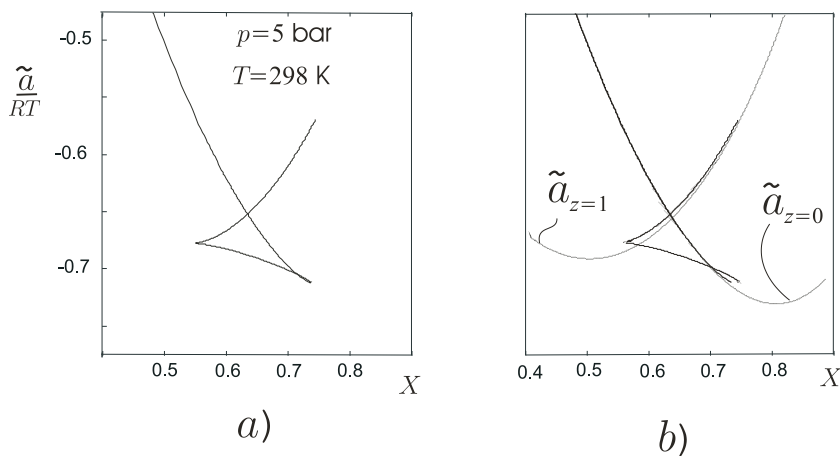


Figure 7: a) The reduced availability for a phase mixture in full equilibrium. b) The dashed curves represent the availability of the pure phases: liquid ($z=1$) and vapor ($z=0$)

concave; it corresponds to the decreasing branch of the $X(z)$ -graph in Fig. 6

3.6 Formation of kernels

For the interpretation of the reduced availability graph in equilibrium it is useful to add the graphs $\tilde{a}_{z=1}(X, p, T)$ from (3.10) and $\tilde{a}_{z=0}(X, p, T)$ from (3.11) to Fig. 7a. This is done in Figs. 7b and 8.

The latter shows the relevant parts of the availabilities \tilde{a}_E , $\tilde{a}_{z=0}$, and $\tilde{a}_{z=1}$ and a number of abscissae to be discussed.

The interpretation of these curves is as follows: In the liquid phase $z = 1$, when X grows away from 0, – by admixing constituent 1 to the pure constituent 2 – the liquid solution begins to compete with a two-phase, liquid-vapor solution at $X = X_{\min}$. But it will remain liquid until it reaches the mol-fraction $X_{1 \rightarrow E}$, because up to that point the two-phase equilibrium has a higher energy than the single liquid phase. The corresponding value $z_{1 \rightarrow E}$ is the phase fraction of a *vapor kernel*, the largest value of z that permits phase equilibrium. The value $z_{1 \rightarrow E}$ may be read off from the descending branch of Fig. 6 as *the* z -value

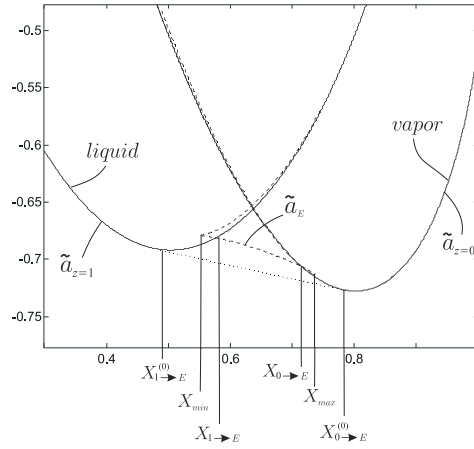


Figure 8: $\tilde{a}_E(X, p, T)$ (dashed) and $\tilde{a}_{z=0}(X, p, T)$, $\tilde{a}_{z=1}(X, p, T)$ (solid) Common tangent for the case without any penalties (dotted)

corresponding to $X = X_{1 \rightarrow E}$. It is noteworthy that the vapor kernel is bounded away from $z = 1$ due to the interface and inhomogeneity penalties; this conclusion follows from Fig. 6 by comparison of the solid and dashed graphs.

Analogously we may start with $z = 0$ in the vapor phase and let X decrease by admixing more and more of constituent 2 to the initially pure constituent 1. The mixture of vapors begins to compete with a two-phase, vapor-liquid solution at $X = X_{\max}$. Yet it will remain in the vapor phase until it reaches the mol fraction $X_{0 \rightarrow E}$, because down to that point the single-phase vapor is energetically more favorable than the two-phase solution. For $X_{0 \rightarrow E}$ the *liquid kernel* appears which has a phase fraction $z_{0 \rightarrow E}$ that may be read off from the descending branch of the $X(z)$ curve of Fig. 6 as the abscissa corresponding to the ordinate value $X_{0 \rightarrow E}$. The smallest kernel has a phase fraction z bounded away from $z = 0$ due to interface and inhomogeneity penalties.

Thus in the range $X_{\min} < X < X_{1 \rightarrow E}$ and $X_{\max} > X > X_{0 \rightarrow E}$ the mixture remains in the liquid and vapor phases respectively. It is true that three minima are available – as explained in the Sect. 3.3 – but the ones for the single phases have lowest energy. The situation is reversed in the range $X_{1 \rightarrow E} < X < X_{0 \rightarrow E}$, because here the two-phase solution has

a smaller energy than either single phase.

The concept of *kernels*, i.e. initial phase fractions bounded away from either $z = 1$ or $z = 0$, has been introduced in the recent paper [5] which deals with interface and inhomogeneity penalties in a single constituent. We may succinctly express the concept by saying that a stable bubble or a stable droplet emerge with a *finite* size. The kernel must not be confused with the unstable nuclei discussed in Sect. 3.4. Indeed in the discussion of the present section the competing energy *minima* determine the phase transition. The nucleation barriers play no role in this discussion; we may think that they are overcome by large enough fluctuations.

We continue the discussion of Fig. 8 with the observation that a vertical line $X = \text{const.}$ with $X_{\min} < X < X_{\max}$ – e.g. $X = 0.6$ – has five points of intersection with the energy curves \tilde{a} and $\tilde{a}_{z=1}, \tilde{a}_{z=0}$. The attentive reader will realize that these points of intersection correspond to the five extrema of the $\tilde{a}(z, X = 0.6)$ curve of Fig. 4. The intersections with the solid lines of Fig. 8 define the end-point minima, while the intersections with the dashed curves define the nucleation barriers and the energy minimum.

To conclude the discussion of Fig. 8 we remark that without any penalties – either due to interfaces or due to non-homogeneity – the concave part of $\tilde{a}(X, p, T)$ stretches into the common tangent of the single-phase availabilities $\tilde{a}_{z=0}(X, p, T)$ and $\tilde{a}_{z=1}(X, p, T)$, while the convex parts of \tilde{a}_E tend to merge with the curves $\tilde{a}_{z=0}$ and $\tilde{a}_{z=1}$. There is no difference in that case between X_{\min} and $X_{1 \rightarrow E}$; both coincide with $X_{1 \rightarrow E}^{(0)}$, cf. Fig. 8. There are no nucleation barriers in this case nor are there kernels, i.e. minimal phase fractions for droplets or bubbles.

Also in the absence of any penalties the dotted curve of Fig. 6 is squeezed into the zig-zag graph defined by the vertical lines $z = 0$ and $z = 1$ and the decreasing solid line.

3.7 Phase diagram for unrestricted miscibility of constituents

It is useful and customary to summarize the foregoing observations in a (p, X) -*phase diagram* which – for a given temperature – represents the

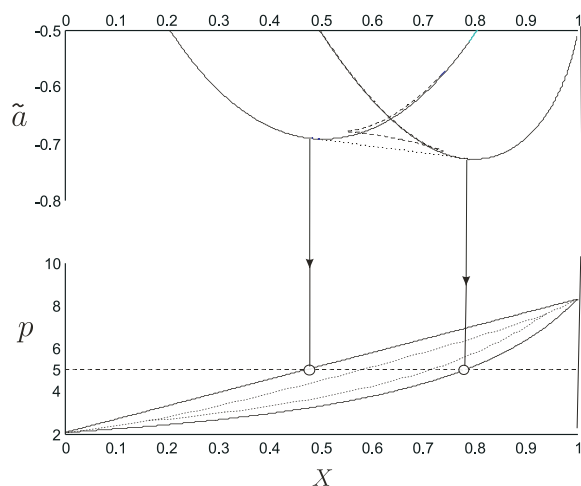


Figure 9: On the construction of a phase diagram with unrestricted miscibility. Solid: without penalties. Dotted: with penalties

lines $p(X; T)$ of the boiling liquid and of the saturated vapor, the so-called boiling line and dew line.

In the case without penalties a pair of points, – one on the boiling line and one on the dew line –, may be obtained by projecting the common tangent of the available free energies $\tilde{a}_{z=1}$ and $\tilde{a}_{z=0}$ onto the appropriate line of constant pressure in a (p, X) -diagram. Fig. 9 illustrates this well-known graphical construction for $p = 5$ bar which produces the two circles; the left one is the boiling point and the right one is the dew point for that pressure.

Since the functions $\tilde{a}_{z=1}$ and $\tilde{a}_{z=0}$ depend on p , cf. (3.10), (3.11), the boiling and dew points shift; the former traces out the boiling line which is a straight line, while the latter traces out the dew line which is part of a hyperbola. For the present case of an ideal solution of incompressible liquids and a mixture of ideal gases the boiling and dew lines may be found analytically for the penalty-free case, e.g. see [7]. The area between the boiling and dew lines is the two-phase, liquid-vapor region.

With the penalty terms we have concluded in the previous section that the boiling starts at $X_{1 \rightarrow E}$ and the condensation starts at $X_{0 \rightarrow E}$, cf. Fig. 8. In Fig. 9 this means that we must project the points of intersection

of \tilde{a}_E with $\tilde{a}_{z=1}$ and $\tilde{a}_{z=0}$ onto the line $p = 5$ bar in the (p, X) -diagram. Thus, we obtain the new boiling and dew points. Between those two points we have a two-phase region which has become smaller. If this construction of boiling and dew points is repeated for different pressures we see the dotted curves appear in Fig. 9. A remarkable phenomenon occurs in dilute solutions as we come close to either $X = 0$ or $X = 1$, or to pressures close to $p_2(T)$ and $p_1(T)$: here the graph of $\tilde{a}_E(X, p)$ lies above the point of intersection between $\tilde{a}_{z=1}$ and $\tilde{a}_{z=0}$ so that it is energetically favorable for the fluid to make a direct transition from liquid to vapor or *vice versa* without an intermediate two-phase region. This is why the two-phase region tapers out to single lines at either end.

4 Phase diagrams with a miscibility gap

4.1 Heat of mixing

We continue to consider the vapor as a mixture of ideal gases, but the liquid solution is now considered non-ideal. Indeed, we assume that the molar Gibbs free energy (3.3) of the liquid phase contains an additional term of the form

$$eX_A(1 - X_A) \quad (e > 0) \quad (4.1)$$

which represents the heat of mixing. Otherwise $g_A(X, p, T)$ is supposed to be unchanged. The heat of mixing renders $g_A(X_A, p, T)$ a non-convex function of X_A , provided that the coefficient e is big enough. In that case, a judicious use of the common-tangent construction provides phase diagrams of the type shown in Fig. 1b, e.g. [7]. The miscibility gap is the projection of the common tangent of the convex parts of $g_A(X_A, p, T)$ for high pressures for which that tangent lies below the common tangents of $g_A(X_A, p, T)$ and $g_B(X_B, p, T)$. We assume that the reader is familiar with that construction in its ordinary form. The most characteristic feature of this phase diagram is the eutectic point, denoted by E in Fig. 1b. E is a triple point, where the vapor phase may coexist with the solutions α and β which are liquids rich and poor, respectively, in constituent 2. The horizontal line through E is called the eutectic line.

We proceed to consider the effect of the interface and inhomogeneity penalties on phase diagrams with a miscibility gap.

4.2 The effect of the heat of mixing on the liquid-vapor equilibrium conditions

The arguments and formulae of Chap. 2 are unaffected when we now take a heat of mixing into account in the liquid phase. And to a certain extent that is true even for the formulae of Chap. 3. In order to avoid repetition we list only those equations that carry a supplementary term and sometimes only that term is written explicitly. Thus (3.1) is unchanged, while the modification in (3.2) is written as

$$\begin{aligned} g_A(X_A, p_A, T) &= (3.2)_1 + eX_A(1 - X_A), \\ g_B(X_B, p_B, T) &= (3.2)_2, \end{aligned} \quad (4.2)$$

meaning that only $(3.2)_1$ acquires an additional term while $(3.2)_2$ is unchanged. The analogues to (3.3) and (3.4) in the present case read

$$\begin{aligned} g_A(p_A, X_A, T) &= X_A [g_1^A(p_1(T), T) + v_1^A(p_A - p_1(T)) \\ &\quad + RT \ln X_A + e(1 - X_A)^2] \\ &\quad + (1 - X_A) [g_2^A(p_2(T), T) \\ &\quad + v_2^A(p_A - p_2(T)) + RT \ln(1 - X_A) + eX_A^2], \\ g_B(p_B, X_B, T) &= (3.4). \end{aligned} \quad (4.3)$$

The chemical potentials μ_α in the two phases assume the forms

$$\begin{aligned} \mu_\alpha^A &= g_\alpha^A(p_\alpha(T), T) + v_\alpha^A(p_A - p_\alpha(T)) \\ &\quad + \begin{cases} RT \ln X_A + e(1 - X_A)^2 & \alpha = 1 \\ RT \ln(1 - X_A) + eX_A^2 & \alpha = 2 \end{cases} \\ \mu_\alpha^B &= (3.5)_2. \end{aligned} \quad (4.4)$$

The reduced availability in mechanical and interfacial equilibrium – defined by the left hand side of (3.9) – may now be written in the form

$$\begin{aligned} \tilde{a} = & z \{ X_A (v_1^A (p_A - p_1(T))) + (1 - X_A) (v_2^A (p_A - p_2(T))) \\ & + e X_A (1 - X_A) + RT (X_A \ln X_A + (1 - X_A) \ln (1 - X_A)) \} \\ & + (1 - z) \left\{ X_B RT \ln \left[\frac{p_B}{p_1(T)} \right] + (1 - X_B) RT \ln \left[\frac{p_B}{p_2(T)} \right] \right. \\ & \left. + RT [X_B \ln X_B + (1 - X_B) \ln (1 - X_B)] \right\}. \end{aligned} \quad (4.5)$$

and in, particular, the reduced availability of the pure phases read

$$\begin{aligned} \tilde{a}_{z=0} &= (3.10) \\ \tilde{a}_{z=1} &= (3.11) + eX(1 - X) \end{aligned} \quad (4.6)$$

The condition of equilibrium of mixing, in addition to mechanical and interface equilibrium assumes the form

$$\begin{aligned} \ln \left(\frac{X_A}{1 - X_A} \frac{1 - X_B}{X_B} \right) + \frac{e}{RT} (1 - 2X_A) = & \ln \frac{p_2(T)}{p_1(T)} + \frac{(p_A - p_2(T)) v_2^A}{RT} \\ & - \frac{(p_A - p_1(T)) v_1^A}{RT} \end{aligned} \quad (4.7)$$

and that condition replaces (3.12).

The final condition for full equilibrium requires that the chemical potentials μ_1^A and μ_1^B be equal, cf. (3.15) and by (4.4) that conditions now reads

$$v_1^A (p_A - p_1(T)) + RT \ln X_A + e(1 - X_A)^2 = RT \ln \frac{p_B}{p_1(T)} + RT \ln X_B. \quad (4.8)$$

With these new equations – including the supplements with e – we must repeat the calculations of Chap. 3 and thus obtain the equilibrium availability \tilde{a}_E and hence the phase diagram for liquid-vapor mixtures.

A typical equilibrium availability, – appropriate for the pressure $p = 9$ bar – is shown in Fig. 10a. Also shown, in Fig. 10a, are the "tangent curves"² between the convex vapor availability $\tilde{a}_{z=0}$ and the right and

²This is what we call – for lack of a better name – the concave curves that replace the common tangents when the penalty terms are taken into account.

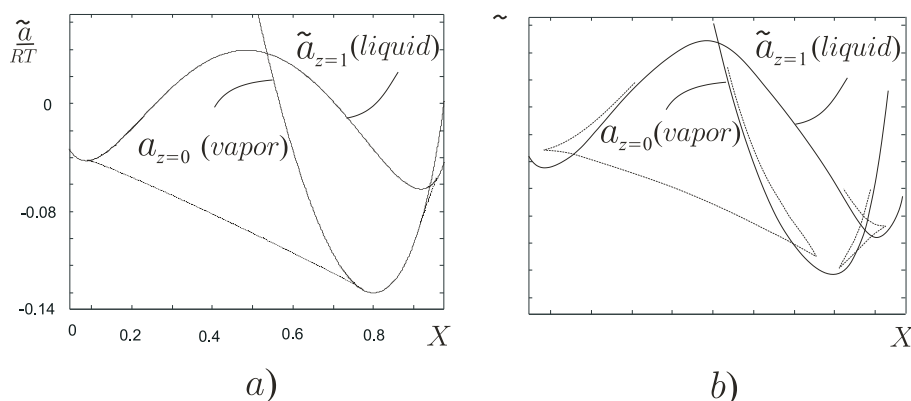


Figure 10: a) The reduced availabilities of the pure phases (solid) and the equilibrium availabilities (dashed) for coexisting liquid and vapor. b) Same as a) with arbitrarily exaggerated differences between equilibrium curves and curves for pure phases

left convex parts of the liquid availability $\tilde{a}_{z=1}$. Since the equilibrium availabilities and the single-phase availabilities in part nearly coincide, we have drawn a schematic picture in Fig. 10b, where the differences are arbitrarily exaggerated.

In order to construct the phase diagram we proceed as indicated in Fig. 9. The novel feature here is that for one pressure we obtain *two* lines of phase equilibrium. For tangents proper this is very well-known and by changing the pressure, we thus obtain the two phase regions α +vapor and β +vapor, cf. Fig. 1b. Of course here, – with tangent *curves* – those regions will be modified as shown in subsequent phase diagrams.

4.3 Heat of mixing produces liquid-liquid phase equilibria

The phase diagram so constructed is not complete, however. Indeed, since the graph of $g_A(X_A, p, T)$ is non-convex, there is the possibility that equilibria between two liquid phases may "interfere" with the equilibria between liquid and vapor; namely in the sense that for some pressure the liquid-liquid phase mixture in a certain range of mol fractions X is en-

ergetically more favorable than the liquid-vapor phase mixture and *vice versa*. That possibility must be investigated and it requires yet another change in the form of our constitutive functions for the Gibbs free energies.

Let A and B now characterize two liquid phases. Thus $g_A(X_A, p, T)$ and $g_B(X_B, p, T)$ both have the form (4.3)₁ with $v_\alpha^A = v_\alpha^B$ ($\alpha = 1, 2$), because the two phases are mixtures of the same incompressible liquids. We have for $I = A, B$ the Gibbs free energies

$$\begin{aligned} g_I(p_I, X_I, T) = & X_I [g_1(p_1(T), T) + v_1(p_I - p_1(T)) \\ & + RT \ln X_I + e(1 - X_I)^2] \\ & + (1 - X_I) [g_2(p_2(T), T) \\ & + v_2(p_I - p_2(T)) + RT \ln(1 - X_I) + eX_I^2], \end{aligned} \quad (4.9)$$

and the chemical potentials

$$\begin{aligned} \mu_1^I(X_I, p_I, T) = & g_1(p_1(T), T) + v_1(p_I - p_1(T)) \\ & + RT \ln X_I + e(1 - X_I)^2 \\ \mu_2^I(X_I, p_I, T) = & g_2(p_2(T), T) + v_2(p_I - p_2(T)) \\ & + RT \ln(1 - X_I) + eX_I^2. \end{aligned} \quad (4.10)$$

The reduced available free energy \tilde{a} for mechanical and interface equilibrium reads in this case

$$\begin{aligned} \tilde{a} = & z \{X_A v_1(p_A - p_1(T)) + (1 - X_A) v_2(p_B - p_2(T)) \\ & + RT [X_A \ln X_A + (1 - X_A) \ln(1 - X_A)] + eX_A(1 - X_A)\} \\ & + (1 - z) \{X_B v_1(p_B - p_1(T)) + (1 - X_B) v_2(p_B - p_2(T)) \\ & + RT [X_B \ln X_B + (1 - X_B) \ln(1 - X_B)] + eX_B(1 - X_B)\}. \end{aligned} \quad (4.11)$$

The single-phase availabilities $\tilde{a}_{z=0}$ and $\tilde{a}_{z=1}$ are equal functions of the variable X in this case, since $p_B = p$ in the former case and $p_A = p$ in the latter. The graph of this function shows a marked non-convexity, if e is chosen big enough. In our calculations e was chosen to be equal to $3RT$.

For equilibrium of mixing, in addition to mechanical and interface equilibrium, the chemical potential differences in the two phases must be

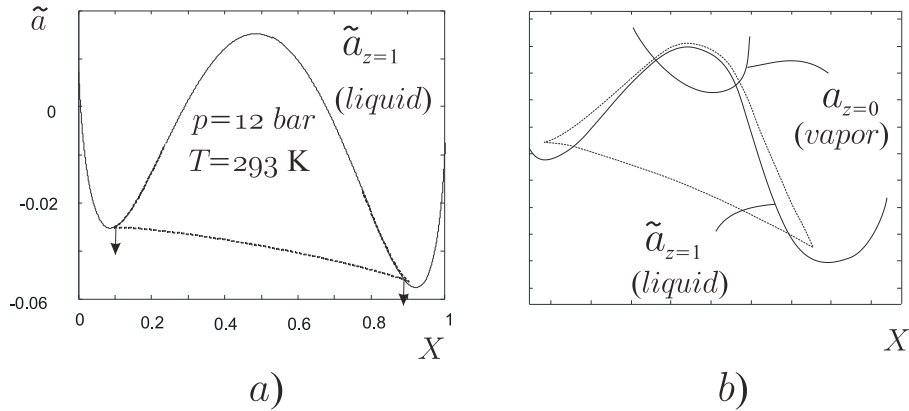


Figure 11: a) Phase equilibrium between the solutions α (left concave part of $\tilde{a}_{z=1}$) and (right concave part). b) Same as a) with arbitrarily exaggerated differences between equilibrium curves and curves for pure phases.

equal and this implies in the present case

$$\ln \left(\frac{X_A}{1-X_A} \frac{1-X_B}{X_B} \right) + \frac{(v_1 - v_2)(p_A - p_B)}{RT} + 2 \frac{e}{RT} (X_B - X_A) = 0. \quad (4.12)$$

For full equilibrium there is one more condition, namely $\mu_1^A = \mu_1^B$ and by (4.10), that condition reads

$$\ln \frac{X_A}{X_B} + \frac{v_1(p_A - p_B)}{RT} + \frac{e}{RT} [(1 - X_A)^2 - (1 - X_B)^2] = 0. \quad (4.13)$$

With these new equations pertaining to two liquid phases we redo the calculations of Chap. 3 and for the high pressure equal to $p = 12$ bar we obtain a "tangent curve" between the two concave parts of the liquid availability. This is shown in Fig. 11a. Fig. 11b shows a schematic picture for a better qualitative understanding.

The projection – indicated by the arrows – of the equilibrium curve on the isobar $p = 12$ bar in a (p, X) -diagram defines the miscibility gap, cf. Fig. 1b. It is clear that the gap is narrowed by the penalty terms, because it costs energy to form interfaces. Also, more formally, the

distance between the arrows in Fig. 11 is smaller than the projection of the common tangent.

Calculations show that the width of the narrowed miscibility gap is practically independent of pressure. This is probably due to the assumption that the two constituents of the mixture are incompressible.

4.4 Phase diagrams with miscibility gap

The situation of low and high pressure shown in Figs. 10 and 11 are qualitatively much like the situation presented in Fig. 9, where the heat of mixing was absent. Complications arise at intermediate pressures when the tangent curves of the liquid-vapor availabilities and of the convex parts of the liquid availability intersect and thereby exchange their roles as minimum energies.

In this range of pressures we register serious modifications of the phase diagram, particularly at the eutectic point and concerning the eutectic line. It is impossible to present all special cases in this paper; they depend on the values of the penalty coefficients τ_1, τ_2 between the liquid phases and between liquids and vapor.

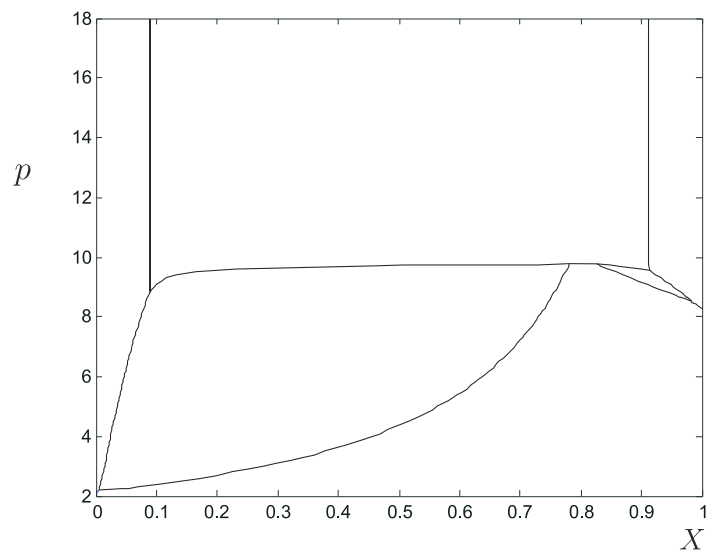
We exhibit some diagrams first and discuss their salient features and how they depend on the values of τ_1 and τ_2 . Afterwards we discuss the complex phase changes at $p = 9.5$ bar as we move horizontally through the phase diagram by admixing more and more of constituent 1.

Fig. 12a shows the case for which all interfaces – the liquid-liquid or liquid-vapor ones – have $\tau_1 = 5 \cdot 10^4$ J, $\tau_2 = 5 \cdot 10^4$ J/m⁹.

In Fig. 12b the same phase diagram is shown again along with the "usual" diagram – dashed – for $\tau_1 = 0, \tau_2 = 0$; this is done for better appreciation of the effects of the interfacial terms.

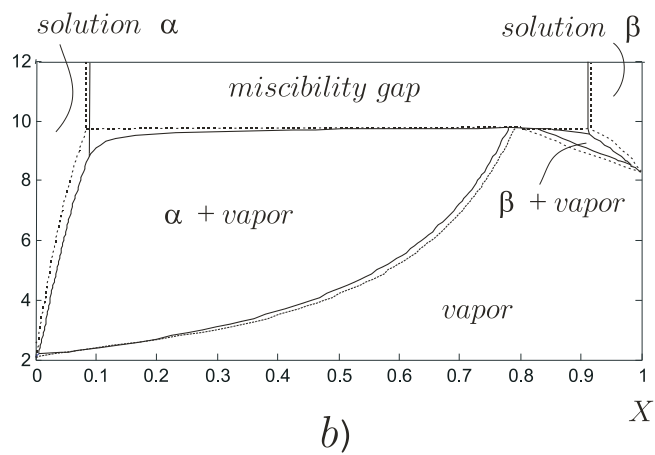
We list some of the salient features:

- The two-phase regions α +vapor and β +vapor taper off into lines as $X = 0$ and $X = 1$ are approached.
- The eutectic point has spread into a short *flat* line.
- The eutectic line is no longer straight



a)

(a) Phase diagrams with miscibility gap. $\tau_1 = 5 \cdot 10^4 J$, $\tau_2 = 5 \cdot 10^4 J/m^9$, $e = 3RT$



b)

(b) Same as a) but with the penalty-free diagram (dashed)

Figure 12:

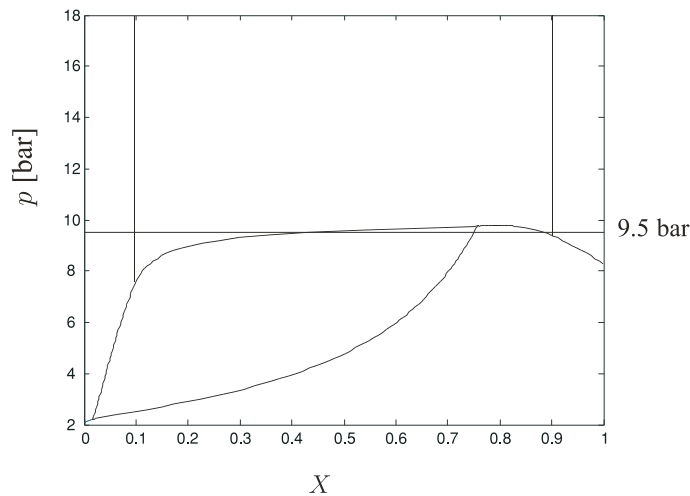


Figure 13: Phase diagram with miscibility gap for large interfacial penalty coefficients

- The two-phase regions have narrowed in width.

Fig. 13 refers to the larger penalty coefficients $\tau_1 = 20 \cdot 10^4$ J, $\tau_2 = 20 \cdot 10^4$ J/m⁹, $e = 3$ and we see that the β +vapor two-phase region has now disappeared. The penalty for the formation of β +vapor interfaces is so great that they do not appear.

The eutectic line has been even more strongly deformed than before and there is a little to remind us of the eutectic point.

Fig. 14 exhibits the diminishing of the β +vapor phase region as the penalty coefficients go up.

So far we have penalized all phase boundaries equally, whether they be of the type α +vapor, β +vapor or $\alpha + \beta$. It is clear that this need not be the case, nor will it be the case in general. In order to illustrate what another choice may result in, we consider the case that there is no interfacial penalty between α and vapor, or between β and vapor, but there is a heavy penalty on interfaces between α and β . In that case we obtain a phase diagram of the form shown in Fig. 15, where the miscibility gap is diminished, because it is heavily penalized. The most visible feature in that figure is that now the eutectic point is drawn out

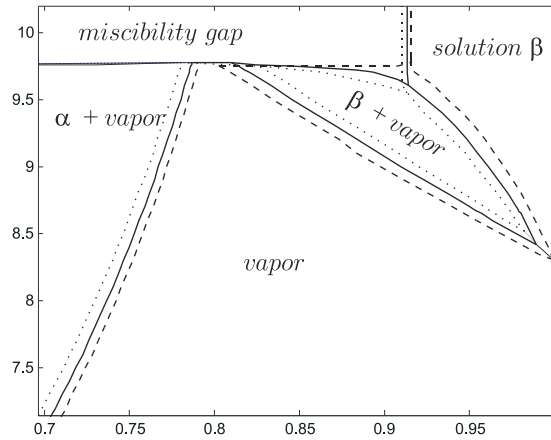


Figure 14: With $(\tau_1, \tau_2) = (0, 0)$ going up to $(2 \cdot 10^4, 2 \cdot 10^4)$ and $(5 \cdot 10^4, 5 \cdot 10^4)$, in the respective units, the β +vapor two-phase region diminishes

into a *steep* line. Upon crossing that line at constant pressure by adding constituent 1 we move from an equilibrium of α -solution and vapor to an equilibrium of β -solution and vapor. Formally what happens is that the common tangent of the left convex part of the liquid and the vapor curve and the common tangent between vapor and the right convex part of the liquid intersect before they reach the vapor curve.

4.5 Study of the 6 phases pertaining to $p = 9.5$ bar

We turn back to Fig. 13 and inspect the phases pertaining to the pressure $p = 9.5$ bar which is indicated in the figure by thin horizontal line. When we start at the point $X = 0$ and admix constituent 1 we pass through 6 phase regions until we reach $X = 1$. The fat dashed and dot-dashed curves in Fig. 16 represent the availabilities of the pure phases vapor and liquid, respectively. The thin curves represent the curves of phase equilibrium. The Roman numbers *I* through *VI* characterize the phases that we pass through in the admixing process as follows.

- *I* – α -solution
- *II* – phase equilibria of $\alpha + \beta$ solutions

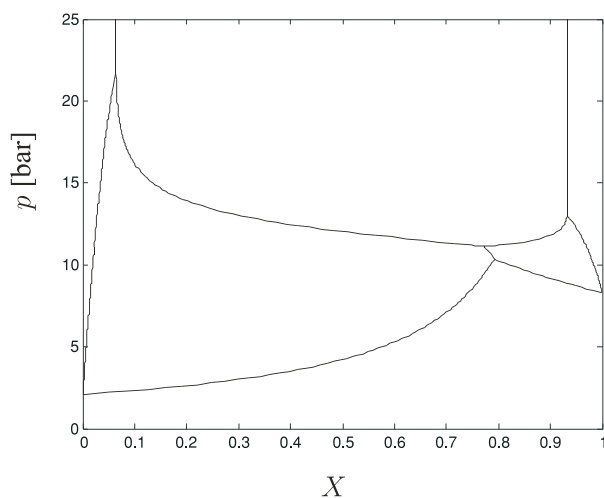


Figure 15: No penalty on α +vapor and β +vapor interfaces. For $\alpha + \beta$ the penalties are $\tau_1 = 441 \cdot 10^4 J$, and $\tau_2 = 441 \cdot 10^4 J/m^9$, $e = 1.4RT$

- *III* – phase equilibrium of α -solution and vapor
- *IV* – vapor phase
- *V* – phase equilibrium of $\alpha + \beta$ solutions (on enlargement in Fig. 16)
- *VI* – β -solution

5 Discussion and criticism

The best-known interfacial phenomena are overheating of a liquid and undercooling of a vapor which delay the liquid-vapor phase transition in a single, or pure fluid beyond the temperature, where the Gibbs free energies of the phases are equal. Analogous effects occur when we try to induce a phase transition by changing the pressure. The phenomenon is due to the fact that it requires energy – the so-called surface energy – to create the surface of a droplet or bubble. The difficulty to overcome

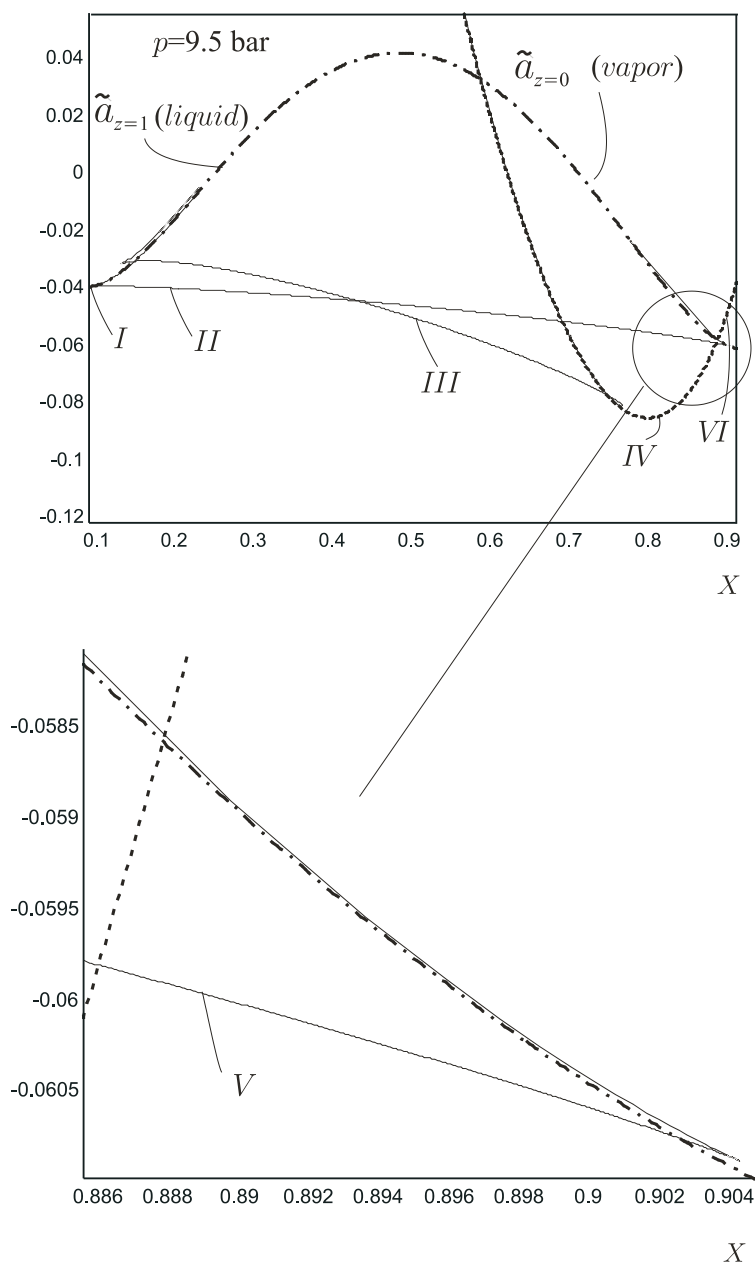


Figure 16: Two phase availabilities for liquid and vapor and equilibrium availabilities for $\alpha + \beta$ equilibrium and $\alpha + \text{vapor}$ equilibrium

the nucleation energy may keep the body in metastable equilibrium. And what we normally perceive as the boiling point or dew point occurs only because the nucleation energy is overcome by the body, either because of large fluctuations or because of the presence of nuclei, i.e. foreign traces that "catalyze" the phase transition. Thus in engineering applications of simple bodies we may often ignore the surface energy and concentrate on the stable equilibria.

The case of solutions is different. We have shown in the foregoing analysis that, even if nucleation barriers and metastable states are ignored, the phase diagrams should exhibit considerable differences from customary ones, e.g. those shown in Figs. 1. Among the predicted differences are

- direct transitions between liquid and vapor for either large or small mol fractions, cf. Figs. 9 or 13. Whenever this occurs, it does occur because the interfacial energy is too big to permit the coexistence of two phases.
- modification of the eutectic point and the eutectic line. The eutectic point in Fig. 1b is a triple point, i.e. a point where three phases may coexist. According to the Gibbs phase rule – applied to a binary solution with fixed temperature – such a three phase coexistence can only occur in isolated points of the phase diagram. However, in Sect. 2.6 we have concluded that the Gibbs rule is modified in the presence of interfacial penalties, because the phase fraction occurs as a relevant variable in the equilibrium conditions. Accordingly we have triple points all along the short steep line separating the α +vapor-region and the β +vapor-region in Fig. 15; those triple equilibria differ by different values of the vapor fraction z .

It may be objected that for our one-dimensional model, which is represented in Fig. 2, it is topologically impossible to have triple points. However, one may argue that the available free energy of equation (2.4) is the true – mathematical – starting point of our model. That equation was *motivated* by Fig. 2 but, as it stands and as it is exploited, it has lost all specific references to one-dimensionality. Thus it permits triple points.

Another valid criticism may demand experimental evidence for the predicted phenomena. We have tried to anticipate such an objection by discussing the subject with chemical engineers and metallurgists. Unfortunately we found it impossible to get through to them even to the extent that we could not successfully communicate the existence of the problem.

Finally we remark that there have been previous attempts to investigate the effect of interfacial penalties upon phase diagrams. These have employed a simpler ansatz than ours by letting the interfacial energy *a priori* be given by the phase fractions. The first such effort was made Cahn and Larché [8], who already remarked on the necessity to reformulate the Gibbs phase rule. The same ansatz was later used by Müller [9], Ansorg & Müller [10] and Ansorg [11]. The results concerning the phase diagram with unrestricted miscibility and the eutectic phase diagram were qualitatively similar to our results.

Acknowledgment: *Three of the authors T.M.A., Z. J., and Y. H. gratefully acknowledge the support of the Alexander von Humboldt Foundation.*

References

- [1] van der Waals, J.D. On the continuity of gaseous and liquid states. Sijthoff, Leiden (1873). Translated and reprinted: Rowlinson, J. S. Studies in Statistical Mechanics **14**, North Holland, Amsterdam (1988).
- [2] van der Waals, J. D. The thermodynamic theory of capillarity under the hypothesis of continuous variation of density. Verhandl. Konik. Akad. Weten. Amsterdam (Sect. 1) **1** (1) (1883).
- [3] Müller, S. Singular perturbations as a selection criterion for periodic minimizing sequences. Calculus of Variations **1**, 169-204 (1993).
- [4] Truskinovsky, L., Zanzotto, G., Finite scale microstructures and metastability in one-dimensional elasticity. Meccanica **30**, 577-589 (1995).
- [5] Huo, Y., Müller, I. Interfacial and inhomogeneity penalties in phase boundaries. Cont. Mech.&Thermodyn. **15**, 395-407 (2003).

- [6] Thomson, W. (Lord Kelvin) Proc. Roy. Soc. Edinburgh **7** (1870)
- [7] Müller, I. Grundzüge der Thermodynamik, Springer Heidelberg 2001.
- [8] Cahn, J. W. and Larché, F. A simple model for coherent equilibria. Acta Metall. **32**, (11) (1984).
- [9] Müller, I. Boiling and Condensation with interfacial energy. Meccanica **31**, (1996).
- [10] Müller, I, Ansorg, J. Phase diagrams, heat of mixing and interfacial energy in : P. Argoül (ed.) Proc. IUTAM Symp. Variations des domaines et frontières en Mécanique des Solides. Kluwer, 1999.
- [11] Ansorg, J. Einführung der Grenzflächenenergie in die Darstellung von Phasenübergängen binärer Mischungen. Dissertation, TU Berlin 2001.

Submitted on October 2007.

Fazni dijagrami modifikovani medjufaznim popravkama

Uobičajeni oblici faznih dijagrama su konstruisani bez razmatranja energija medjupovrši što predstavlja značajni alat za inženjere hemijske i metalurške specijalnosti. Ako se energije medjupovrši uzmu u obzir, tada je intuitivno očigledno da oblasti faznih ravnoteža moraju postati manje jer postoji popravka na formiranje medjupovrši. Ova pojava se proučava kvalitativno za jednodimenzioni model u kojem se faze pojavljuju pre kao slojevi, a ne kao kapljice ili mehurići. Modifikovani fazni dijagrami su prikazani u trećem i četvrtom odeljku rada.